DESY 95-148
UdeM-GPP-TH-95-32

CP Violation and Flavour Mixing in the Standard Model

A. Ali*

Deutsches Elektronen Synchrotron DESY, Hamburg

and

D. London

Laboratoire de physique nucléaire, Université de Montréal
C.P. 6128, succ. centre-ville, Montréal, QC, Canada H3C 3J7

Abstract

We review and update the constraints on the parameters of the quark flavour mixing matrix V_{CKM} in the standard model and estimate the resulting CP asymmetries in B decays, taking into account recent experimental and theoretical developments. In performing our fits, we use inputs from the measurements of the following quantities: (i) $|\epsilon|$, the CP-violating parameter in K decays, (ii) ΔM_d, the mass difference due to the B^0_d-$\overline{B^0_d}$ mixing, (iii) the matrix elements $|V_{cb}|$ and $|V_{ub}|$, (iv) B-hadron lifetimes, and (v) the top quark mass. The experimental input in points (ii) - (v) has improved compared to our previous fits. With the updated CKM matrix we present the currently-allowed range of the ratios $|V_{td}/V_{ts}|$ and $|V_{td}/V_{ub}|$, as well as the standard model predictions for the B^0_s-$\overline{B^0_s}$ mixing parameter x_s (or, equivalently, ΔM_s) and the quantities $\sin 2\alpha$, $\sin 2\beta$ and $\sin^2\gamma$, which characterize the CP-asymmetries in B-decays. Various theoretical issues related to the so-called "penguin-pollution," are of importance for the determination of the phases α and γ from the CP-asymmetries in B decays, are also discussed.

*Presented at the 6th. International Symposium on Heavy Flavour Physics, Pisa, June 6 - 10, 1995.

1 Introduction

The aim of this article is to revise and update the profile of the Cabibbo-Kobayashi-Maskawa (CKM) matrix reported earlier by us [1], in particular the CKM unitarity triangle and the CP asymmetries in B decays, which are the principal objects of interest in experiments at present and forthcoming B facilities. In performing this update, we include the improvements reported in a number of measurements of the lifetime, mixing ratio, and the CKM matrix elements $|V_{cb}|$ and $|V_{ub}/V_{cb}|$ from B decays, as well as the top quark mass. On the theoretical side, we mention the improved estimates of the power corrections in the analysis of the exclusive semileptonic decay $B \to D^* \ell \nu_\ell$ in the context of the heavy quark effective theory (HQET) [2, 3], and the calculation of the missing part of the next-to-leading order calculations in the analysis of the CP-violating quantity $|\epsilon|$ [4]. We note here the changes that we have made in the input to our present analysis compared to that reported by us in Ref. [1]:

- The top quark (pole) mass $m_t = 174 \pm 16$ GeV, measured earlier by the CDF collaboration [5], is now replaced by improved measurements by the same collaboration [6] and by D0 [7], yielding the present world average $m_t = 180 \pm 11$ GeV [8]. This leads to the running top quark mass in the $\overline{MS}$ scheme, $\overline{m_t}(m_t) = 170 \pm 11$ GeV [9].

- A new and improved measurement of the quantity $\mathcal{F}(1)|V_{cb}|$ in the decays $B \to D^* \ell \nu_\ell$, using methods based on the heavy quark effective theory (HQET), has been reported by the ALEPH collaboration [10]. This is lower than their previous number [11], as well as the corresponding numbers from the CLEO [12] and ARGUS [13] analyses. Likewise, new measurements are reported by the DELPHI collaboration [14]. In the meantime, estimates for the quantity $\mathcal{F}(1) \equiv \xi(1)\eta_A$ have undergone some revision in both the QCD perturbative part η_A and power corrections to the Isgur-Wise function at the symmetry point $\xi(1)$. We use the value $\mathcal{F}(1) = 0.91 \pm 0.04$, obtained recently by Neubert [2], and which is in good agreement with the estimates of Shifman et al. [3, 15]. Taking into account the updated experimental and theoretical input, we obtain $|V_{cb}| = 0.0388 \pm 0.0036$. The central value for this matrix element has come down compared to the value $|V_{cb}| = 0.041 \pm 0.006$ used by us previously, and the error on this quantity is now smaller, about $\pm 9\%$.

- Until recently, the knowledge of the CKM matrix element ratio $|V_{ub}/V_{cb}|$ was based on the analysis of the end-point lepton energy spectrum in semileptonic B decays [16], which is quite model-dependent. We had used a value $|V_{ub}/V_{cb}| = 0.08 \pm 0.03$ to take this model dependence into account. In the meantime, the measurement of the exclusive semileptonic decays $B \to (\pi, \rho)\ell\nu_\ell$ has been reported by the CLEO collaboration [17]. The matrix element ratio so determined is also model-dependent due to the decay form factors. However, this set of data permits a discrimination among a number of models, all of which were previously allowed from the inclusive decay analysis. The convolution of the two methods reduces the theoretical uncertainty somewhat. We use a value $|V_{ub}/V_{cb}| = 0.08 \pm 0.02$, which is a fair reflection of the underlying present theoretical dispersion on this ratio.

- In the analysis of the CP-violating quantity $|\epsilon|$, the perturbative renormalizations of the various pieces in the $|\Delta S| = 2$ Hamiltonian from the intermediate charm and top quark are required [18]. While the next-to-leading order results for the quantities $\hat{\eta}_{cc}$ and $\hat{\eta}_{tt}$ have been known for some time and were used in our previous analysis, the next-to-leading order calculation of the quantity $\hat{\eta}_{ct}$ has been completed only recently [4]. We use the improved calculation of $\hat{\eta}_{ct}$ in performing the CKM fits presented here.

- The measurements of the B_d^0-$\overline{B_d^0}$ mass difference ΔM_d have become quite precise, with the present world average being $\Delta M_d = 0.465 \pm 0.024\ (ps)^{-1}$ [19]. The present lower limit on the B_s^0-$\overline{B_s^0}$ mass difference has improved slightly, $\Delta M_s > 6.1\ (ps)^{-1}$ at 95 % C.L., assuming for the probability of the fragmentation of a b quark into a B_s meson a value $f_s = 12\%$ [20], yielding $\Delta M_s/\Delta M_d > 12.3$ at 95% C.L. [19].

All of these improvements warrant an updated fit of the CKM parameters.

As in our previous analysis, we consider two types of fits. In Fit 1, we assume particular fixed values for the theoretical hadronic quantities. The allowed ranges for the CKM parameters are derived from the (Gaussian) errors on experimental measurements only. In Fit 2, we assign a central value plus an error (treated as Gaussian) to the theoretical quantities. In the resulting fits, we combine the experimental and theoretical errors in quadrature. For both fits we calculate the allowed region in CKM parameter space at 95% C.L. We also estimate the SM prediction for the B_s^0-$\overline{B_s^0}$ mixing parameter, x_s, and show how the ALEPH limit of $\Delta M_s/\Delta M_d > 12.3$ (95% C.L.) constrains the CKM parameter space. We give the present 95% C.L. upper and lower bounds on the matrix element ratio $|V_{td}/V_{ts}|$, as well as the allowed (correlated) values of the CKM matrix elements $|V_{td}|$ and $|V_{ub}|$.

We also present the corresponding allowed ranges for the CP-violating phases that will be measured in B decays, characterized by $\sin 2\beta$, $\sin 2\alpha$ and $\sin^2\gamma$. These can be measured directly through rate asymmetries in the decays $\overset{(-)}{B}{}_d^0 \to J/\psi K_S$, $\overset{(-)}{B}{}_d^0 \to \pi^+\pi^-$, and $\overset{(-)}{B}{}_s^0 \to D_s^{\pm}K^{\mp}$ (or $B^{\pm} \to \overset{(-)}{D}{}^0 K^{\pm}$), respectively. We also give the allowed domains for two of the angles, $(\sin 2\alpha, \sin 2\beta)$. Finally, we briefly discuss the role of penguins (strong and electroweak) in extracting the CP phases α and γ from the measurements of various CP-asymmetries.

This paper is organized as follows. In Section 2, we present our update of the CKM matrix, concentrating especially on the matrix element $|V_{cb}|$ which, thanks to the progress in HQET and experiments, is now well under control. The constraints that follow from $|V_{ub}/V_{cb}|$, $|\epsilon|$ and ΔM_d on the CKM parameters are also discussed here. Section 3 contains the results of our fits. These results are summarized in terms of the allowed domains of the unitarity triangle, which are displayed in several figures and tables. In Section 4, we discuss the impact of the recent lower limit on the ratio $\Delta M_s/\Delta M_d$ reported by the ALEPH collaboration on the CKM parameters and estimate the expected range of the mixing ratio x_s in the SM based on our fits. Here we also present the allowed 95% C.L. range for $|V_{td}/V_{ts}|$. In Section 5 we discuss the predictions for the CP asymmetries in the neutral B meson sector and calculate the correlations for the CP violating asymmetries proportional to $\sin 2\alpha$, $\sin 2\beta$ and $\sin^2\gamma$. We also review some of the possible theoretical

uncertainties in extracting these CP-phases due to the presence of strong and/or electroweak penguins. We present here the allowed values of the CKM matrix elements $|V_{td}|$ and $|V_{ub}|$. Section 6 contains a summary and an outlook for improving the profile of the CKM unitarity triangle.

2 An Update of the CKM Matrix

In updating the CKM matrix elements, we make use of the Wolfenstein parametrization [21], which follows from the observation that the elements of this matrix exhibit a hierarchy in terms of λ, the Cabibbo angle. In this parametrization the CKM matrix can be written approximately as

$$V_{CKM} \simeq \begin{pmatrix} 1-\frac{1}{2}\lambda^2 & \lambda & A\lambda^3(\rho - i\eta) \\ -\lambda(1+iA^2\lambda^4\eta) & 1-\frac{1}{2}\lambda^2 & A\lambda^2 \\ A\lambda^3(1-\rho-i\eta) & -A\lambda^2 & 1 \end{pmatrix} . \tag{1}$$

In this section we shall discuss those quantities which constrain these CKM parameters, pointing out the significant changes in the determination of λ, A, ρ and η.

We recall that $|V_{us}|$ has been extracted with good accuracy from $K \to \pi e\nu$ and hyperon decays [22] to be

$$|V_{us}| = \lambda = 0.2205 \pm 0.0018 . \tag{2}$$

This agrees quite well with the determination of $V_{ud} \simeq 1 - \frac{1}{2}\lambda^2$ from β-decay,

$$|V_{ud}| = 0.9744 \pm 0.0010 . \tag{3}$$

The parameter A is related to the CKM matrix element V_{cb}, which can be obtained from semileptonic decays of B mesons. We shall restrict ourselves to the methods based on HQET to calculate the exclusive and inclusive semileptonic decay rates. In the heavy quark limit it has been observed that all hadronic form factors in the semileptonic decays $B \to (D, D^*)\ell\nu_\ell$ can be expressed in terms of a single function, the Isgur-Wise function [23]. It has been shown that the HQET-based method works best for $B \to D^* l\nu$ decays, since these are unaffected by $1/m_Q$ corrections [24, 25, 26]. This method has been used by the ALEPH, ARGUS, CLEO and DELPHI collaborations to determine $\xi(1)|V_{cb}|$ and the slope of the Isgur-Wise function.

Using HQET, the differential decay rate in $B \to D^*\ell\nu_\ell$ is

$$\begin{aligned} \frac{d\Gamma(B \to D^*\ell\bar{\nu})}{d\omega} &= \frac{G_F^2}{48\pi^3}(m_B - m_{D^*})^2 m_{D^*}^3 \eta_A^2 \sqrt{\omega^2-1}(\omega+1)^2 \\ &\quad \times [1 + \frac{4\omega}{\omega+1}\frac{1-2\omega r + r^2}{(1-r)^2}]|V_{cb}|^2\xi^2(\omega) , \end{aligned} \tag{4}$$

where $r = m_{D^*}/m_B$, $\omega = v \cdot v'$ (v and v' are the four-velocities of the B and D^* meson, respectively), and η_A is the short-distance correction to the axial vector form factor. In the leading logarithmic approximation, this was calculated by Shifman and Voloshin some time ago – the so-called hybrid anomalous dimension [27]. In the absence of any power

corrections, $\xi(\omega = 1) = 1$. The size of the $O(1/m_b^2)$ and $O(1/m_c^2)$ corrections to the Isgur-Wise function, $\xi(\omega)$, and partial next-to-leading order corrections to η_A have received a great deal of theoretical attention, and the state of the art has been summarized recently by Neubert [2] and Shifman [3]. Following them, we take:

$$\begin{aligned} \xi(1) &= 1 + \delta(1/m^2) = 0.945 \pm 0.025 \ , \\ \eta_A &= 0.965 \pm 0.020 \ . \end{aligned} \tag{5}$$

This gives the range [2]:

$$\mathcal{F}(1) = 0.91 \pm 0.04 \ . \tag{6}$$

The present experimental input from the exclusive semileptonic channels is based on the data by CLEO [12], ALEPH [10], ARGUS [13], and DELPHI [14]:

$$\begin{aligned} |V_{cb}| \cdot \mathcal{F}(1) &= 0.0351 \pm 0.0019 \pm 0.0020 \quad \text{[CLEO]}, \\ &= 0.0314 \pm 0.0023 \pm 0.0025 \quad \text{[ALEPH]}, \\ &= 0.0388 \pm 0.0043 \pm 0.0025 \quad \text{[ARGUS]}, \\ &= 0.0374 \pm 0.0021 \pm 0.0034 \quad \text{[DELPHI]}, \end{aligned} \tag{7}$$

where the first error is statistical and the second systematic. The ARGUS number has been updated by taking into account the updated lifetimes for the B^0 and $B^\pm$ mesons [28]. The statistically weighted average of these numbers is:

$$|V_{cb}| \cdot \mathcal{F}(1) = 0.0353 \pm 0.0018 \ , \tag{8}$$

which, using $\mathcal{F}(1)$ from Eq. (6), gives the following value:

$$|V_{cb}| = 0.0388 \pm 0.0019 \ (expt) \pm 0.0017 \ (th). \tag{9}$$

Combining the errors linearly gives $|V_{cb}| = 0.0388 \pm 0.0036$. This is in good agreement with the value $|V_{cb}| = 0.037^{+0.003}_{-0.002}$ obtained from the exclusive decay $B \to D^* \ell \nu_\ell$, using a dispersion relation approach [29]. Likewise, the value of $|V_{cb}|$ obtained from the inclusive semileptonic B decays using HQET is quite compatible with the above determination [16]:

$$|V_{cb}| = 0.040 \pm 0.0010 \ (expt) \pm 0.005 \ (th) \ . \tag{10}$$

In the fits below we shall use $|V_{cb}| = 0.0388 \pm 0.0036$, yielding

$$A = 0.80 \pm 0.075 \ . \tag{11}$$

The other two CKM parameters ρ and η are constrained by the measurements of $|V_{ub}/V_{cb}|$, $|\epsilon|$ (the CP-violating parameter in the kaon system), x_d (B_d^0-$\overline{B_d^0}$ mixing) and (in principle) ϵ'/ϵ ($\Delta S = 1$ CP-violation in the kaon system). We shall not discuss the constraints from ϵ'/ϵ, due to the various experimental and theoretical uncertainties surrounding it at present, but take up the rest in turn and present fits in which the allowed region of ρ and η is shown.

Up to now, $|V_{ub}/V_{cb}|$ was obtained by looking at the endpoint of the inclusive lepton spectrum in semileptonic B decays. Unfortunately, there still exists quite a bit of model

dependence in the interpretation of the inclusive data by themselves. As mentioned earlier, a recent new input to this quantity is provided by the measurements of the exclusive semileptonic decays $B \to (\pi, \rho)\ell\nu_\ell$. The ratios of the exclusive semileptonic branching ratios provide some discrimination among the various models [17]. In particular, models such as that of Isgur et al. [30], which give values in excess of 3 for the ratio of the decay widths $\Gamma(B^0 \to \rho^-\ell^+\nu)/\Gamma(B^0 \to \pi^-\ell^+\nu)$, are disfavoured by the CLEO data. The disfavoured models are also those which introduce a larger theoretical dispersion in the interpretation of the inclusive $B \to X_u\ell\nu_\ell$ and exclusive decay data in terms of the ratio $|V_{ub}/V_{cb}|$. Excluding them from further consideration, measurements in both the inclusive and exclusive modes are compatible with

$$\left|\frac{V_{ub}}{V_{cb}}\right| = 0.08 \pm 0.02 \ . \tag{12}$$

This gives

$$\sqrt{\rho^2+\eta^2} = 0.36 \pm 0.08 \ . \tag{13}$$

With the measurements of the form factors in semileptonic decays $B \to (\pi, \rho, \omega)\ell\nu_\ell$, one should be able to further constrain the models, thereby reducing the present theoretical uncertainty on this quantity.

The experimental value of $|\epsilon|$ is [22]

$$|\epsilon| = (2.26 \pm 0.02) \times 10^{-3} \ . \tag{14}$$

Theoretically, $|\epsilon|$ is essentially proportional to the imaginary part of the box diagram for K^0-$\overline{K^0}$ mixing and is given by [31]

$$\begin{aligned} |\epsilon| \ &= \ \frac{G_F^2 f_K^2 M_K M_W^2}{6\sqrt{2}\pi^2 \Delta M_K} \hat{B}_K \left(A^2\lambda^6\eta\right) \left(y_c \left\{\hat{\eta}_{ct} f_3(y_c, y_t) - \hat{\eta}_{cc}\right\}\right. \\ &\left. + \ \hat{\eta}_{tt} y_t f_2(y_t) A^2\lambda^4(1-\rho)\right), \end{aligned} \tag{15}$$

where $y_i \equiv m_i^2/M_W^2$, and the functions f_2 and f_3 can be found in Ref. [1]. Here, the $\hat{\eta}_i$ are QCD correction factors, of which $\hat{\eta}_{cc}$ [32] and $\hat{\eta}_{tt}$ [33] were calculated some time ago to next-to-leading order, and $\hat{\eta}_{ct}$ was known only to leading order [18, 34]. Recently, this last renormalization constant was also calculated to next-to-leading order [4]. We use the following values for the renormalization-scale-invariant coefficients: $\hat{\eta}_{cc} \simeq 1.32$, $\hat{\eta}_{tt} \simeq 0.57$, $\hat{\eta}_{ct} \simeq 0.47$, calculated for $\hat{m}_c = 1.3$ GeV and the NLO QCD parameter $\Lambda_{\overline{MS}} = 310$ MeV in Ref. [4].

The final parameter in the expression for $|\epsilon|$ is the renormalization-scale independent parameter $\hat{B}_K$, which represents our ignorance of the hadronic matrix element $\langle K^0|(\overline{d}\gamma^\mu(1-\gamma_5)s)^2|\overline{K^0}\rangle$. The evaluation of this matrix element has been the subject of much work. The earlier results are summarized in Ref. [35].

In our first set of fits, we consider specific values in the range 0.4 to 1.0 for $\hat{B}_K$. As we shall see, for $\hat{B}_K = 0.4$ a very poor fit to the data is obtained, so that such small values are quite disfavoured. In Fit 2, we assign a central value plus an error to $\hat{B}_K$. As in our previous analysis [1], we consider two ranges for $\hat{B}_K$:

$$\hat{B}_K = 0.8 \pm 0.2 \ , \tag{16}$$

which reflects the estimates of this quantity in lattice QCD [36, 37], or

$$\hat{B}_K = 0.6 \pm 0.2 \ , \tag{17}$$

which overlaps with the values suggested by chiral perturbation theory [38]. As we will see, there is not an enormous difference in the results for the two ranges.

We now turn to B^0_d-$\overline{B^0_d}$ mixing. The present world average of $x_d \equiv \Delta M_d/\Gamma_d$, which is a measure of this mixing, is [19]

$$x_d = 0.73 \pm 0.04 \ , \tag{18}$$

which is based on time-integrated measurements which directly measure x_d, and on time-dependent measurements which measure the mass difference ΔM_d directly. This is then converted to x_d using the B^0_d lifetime, which is known very precisely ($\tau(B_d) = 1.57 \pm 0.05\ ps$). From a theoretical point of view it is better to use the mass difference ΔM_d, as it liberates one from the errors on the lifetime measurement. In fact, the present precision on ΔM_d, pioneered by time-dependent techniques at LEP, is quite competitive with the precision on x_d. The LEP average for ΔM_d has been combined with that derived from time-integrated measurements yielding the present world average [19]

$$\Delta M_d = 0.465 \pm 0.024 \ (ps)^{-1} \ . \tag{19}$$

We shall use this number instead of x_d, which has been the usual practice to date [18, 35, 38, 39].

The mass difference ΔM_d is calculated from the B^0_d-$\overline{B^0_d}$ box diagram. Unlike the kaon system, where the contributions of both the c- and the t-quarks in the loop were important, this diagram is dominated by t-quark exchange:

$$\Delta M_d = \frac{G_F^2}{6\pi^2} M_W^2 M_B \left(f_{B_d}^2 \hat{B}_{B_d} \right) \hat{\eta}_B y_t f_2(y_t) |V_{td}^* V_{tb}|^2 \ , \tag{20}$$

where, using Eq. 1, $|V_{td}^* V_{tb}|^2 = A^2\lambda^6 \left[(1-\rho)^2 + \eta^2 \right]$. Here, $\hat{\eta}_B$ is the QCD correction. In Ref. [33], this correction is analyzed including the effects of a heavy t-quark. It is found that $\hat{\eta}_B$ depends sensitively on the definition of the t-quark mass, and that, strictly speaking, only the product $\hat{\eta}_B(y_t) f_2(y_t)$ is free of this dependence. In the fits presented here we use the value $\hat{\eta}_B = 0.55$, calculated in the $\overline{MS}$ scheme, following Ref. [33]. Consistency requires that the top quark mass be rescaled from its pole (mass) value of $m_t = 180 \pm 11$ GeV to the value $\overline{m_t}(m_t(pole))$ in the $\overline{MS}$ scheme, which is typically about 10 GeV smaller [9].

For the B system, the hadronic uncertainty is given by $f_{B_d}^2 \hat{B}_{B_d}$, analogous to $\hat{B}_K$ in the kaon system, except that in this case, also f_{B_d} is not measured. In our fits, we will take ranges for $f_{B_d}^2 \hat{B}_{B_d}$ and $\hat{B}_{B_d}$ which are compatible with results from both lattice-QCD and QCD sum rules [36, 40, 41]:

$$\begin{aligned} f_{B_d} &= 180 \pm 50 \text{ MeV} \ , \\ \hat{B}_{B_d} &= 1.0 \pm 0.2 \ . \end{aligned} \tag{21}$$

In Table 1, we summarize all input quantities to our fits, of which seven quantities ($|V_{cb}|$, $|V_{ub}/V_{cb}|$, ΔM_d, $\tau(B_d)$, $\overline{m_t}$, $\hat{\eta}_{cc}$, $\hat{\eta}_{ct}$) have changed compared to their values used in our previous fit [1].

Parameter	Value
λ	0.2205
$\|V_{cb}\|$	0.0388 ± 0.0036
$\|V_{ub}/V_{cb}\|$	0.08 ± 0.02
$\|\epsilon\|$	$(2.26 \pm 0.02) \times 10^{-3}$
ΔM_d	$(0.465 \pm 0.024)\ (ps)^{-1}$
$\tau(B_d)$	$(1.57 \pm 0.05)\ (ps)$
$\overline{m_t}(m_t(pole))$	(170 ± 11) GeV
$\hat{\eta}_B$	0.55
$\hat{\eta}_{cc}$	1.32
$\hat{\eta}_{ct}$	0.47
$\hat{\eta}_{tt}$	0.57
$\hat{B}_K$	0.8 ± 0.2
$\hat{B}_B$	1.0 ± 0.2
f_{B_d}	180 ± 50 MeV

Table 1: Parameters used in the CKM fits. Values of the hadronic quantities f_{B_d}, $\hat{B}_{B_d}$ and $\hat{B}_K$ shown are motivated by the lattice QCD results. In Fit 1, specific values of these hadronic quantities are chosen, while in Fit 2, they are allowed to vary over the given ranges. (In Fit 2, for comparison we also consider the range $\hat{B}_K = 0.6 \pm 0.2$, which is motivated by chiral perturbation theory and QCD sum rules.)

3 The Unitarity Triangle

The allowed region in ρ-η space can be displayed quite elegantly using the so-called unitarity triangle. The unitarity of the CKM matrix leads to the following relation:

$$V_{ud}V_{ub}^* + V_{cd}V_{cb}^* + V_{td}V_{tb}^* = 0 \ . \tag{22}$$

Using the form of the CKM matrix in Eq. 1, this can be recast as

$$\frac{V_{ub}^*}{\lambda V_{cb}} + \frac{V_{td}}{\lambda V_{cb}} = 1 \ , \tag{23}$$

which is a triangle relation in the complex plane (i.e. ρ-η space), illustrated in Fig. 1. Thus, allowed values of ρ and η translate into allowed shapes of the unitarity triangle.

In order to find the allowed unitarity triangles, the computer program MINUIT is used to fit the CKM parameters A, ρ and η to the experimental values of $|V_{cb}|$, $|V_{ub}/V_{cb}|$, $|\epsilon|$ and x_d. Since λ is very well measured, we have fixed it to its central value given above. As discussed in the introduction, we present here two types of fits:

- Fit 1: the "experimental fit." Here, only the experimentally measured numbers are used as inputs to the fit with Gaussian errors; the coupling constants $f_{B_d}\sqrt{\hat{B}_{B_d}}$ and $\hat{B}_K$ are given fixed values.

- Fit 2: the "combined fit." Here, both the experimental and theoretical numbers are used as inputs assuming Gaussian errors for the theoretical quantities.

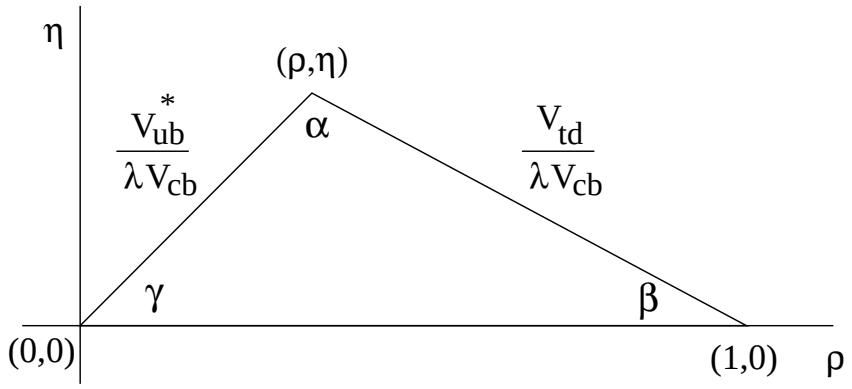

Figure 1: The unitarity triangle. The angles α, β and γ can be measured via CP violation in the B system.

We first discuss the "experimental fit" (Fit 1). The goal here is to restrict the allowed range of the parameters (ρ, η) for given values of the coupling constants $f_{B_d}\sqrt{\hat{B}_{B_d}}$ and $\hat{B}_K$. For each value of $\hat{B}_K$ and $f_{B_d}\sqrt{\hat{B}_{B_d}}$, the CKM parameters A, ρ and η are fit to the experimental numbers given in Table 1 and the χ^2 is calculated.

First, we fix $\hat{B}_K = 0.8$, and vary $f_{B_d}\sqrt{\hat{B}_{B_d}}$ in the range 130 MeV to 230 MeV. The fits are presented as an allowed region in ρ-η space at 95% C.L. ($\chi^2 = \chi^2_{min} + 6.0$). The results are shown in Fig. 2. As we pass from Fig. 2(a) to Fig. 2(e), the unitarity triangles represented by these graphs become more and more obtuse. Even more striking than this, however, is the fact that the range of possibilities for these triangles is quite large. There are two things to be learned from this. First, our knowledge of the unitarity triangle is at present rather poor. This will be seen even more clearly when we present the results of Fit 2. Second, unless our knowledge of hadronic matrix elements improves considerably, measurements of $|\epsilon|$ and x_d, no matter how precise, will not help much in further constraining the unitarity triangle. This is why measurements of CP-violating rate asymmetries in the B system are so important [42, 43]. Being largely independent of theoretical uncertainties, they will allow us to accurately pin down the unitarity triangle. With this knowledge, we could deduce the correct values of $\hat{B}_K$ and $f_{B_d}\sqrt{\hat{B}_{B_d}}$, and thus rule out or confirm different theoretical approaches to calculating these hadronic quantities.

Despite the large allowed region in the ρ-η plane, certain values of $\hat{B}_K$ and $f_{B_d}\sqrt{\hat{B}_{B_d}}$ are disfavoured since they do not provide a good fit to the data. For example, fixing $\hat{B}_K = 1.0$, we can use the fitting program to provide the minimum χ^2 for various values of $f_{B_d}\sqrt{\hat{B}_{B_d}}$. The results are shown in Table 2, along with the best fit values of (ρ, η). Since we have two variables (ρ and η), we use $\chi^2_{min} < 2.0$ as our "good fit" criterion, and we see that $f_{B_d}\sqrt{\hat{B}_{B_d}} < 130$ MeV and $f_{B_d}\sqrt{\hat{B}_{B_d}} > 270$ MeV give poor fits to the existing data. Note also that the χ^2 distribution has two minima, at around $f_{B_d}\sqrt{\hat{B}_{B_d}} = 150$ and 230 MeV. We do not consider this terribly significant, since the surrounding values of $f_{B_d}\sqrt{\hat{B}_{B_d}}$ also yield good fits to the data. The very small values of χ^2_{min} depend sensitively on the central values of the various experimental quantities – if these values move around a little

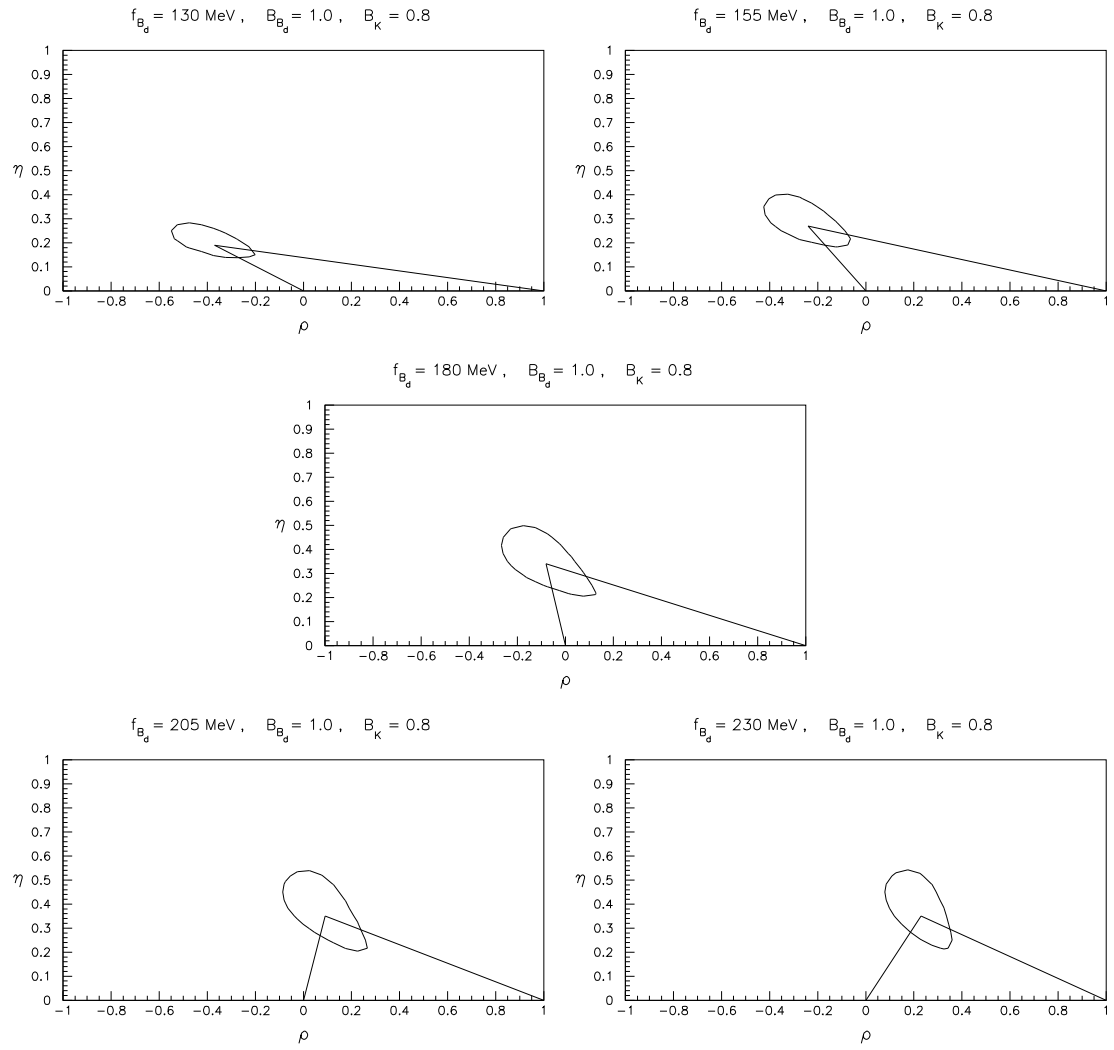

Figure 2: Allowed region in ρ-η space, from a fit to the experimental values given in Table 1. We have fixed $\hat{B}_K = 0.8$ and vary the coupling constant product $f_{B_d}\sqrt{\hat{B}_{B_d}}$ as indicated on the figures. The solid line represents the region with $\chi^2 = \chi^2_{min} + 6$ corresponding to the 95% C.L. region. The triangles show the best fit.

$f_{B_d}\sqrt{\hat{B}_{B_d}}$ (MeV)	(ρ, η)	χ^2_{min}
120	$(-0.43,\ 0.13)$	2.89
130	$(-0.38,\ 0.16)$	1.16
140	$(-0.34,\ 0.18)$	0.3
150	$(-0.30,\ 0.21)$	9.2×10^{-3}
160	$(-0.25,\ 0.24)$	0.07
170	$(-0.20,\ 0.27)$	0.29
180	$(-0.14,\ 0.29)$	0.52
190	$(-0.07,\ 0.31)$	0.64
200	$(0.0,\ 0.31)$	0.59
210	$(0.07,\ 0.31)$	0.38
220	$(0.13,\ 0.31)$	0.13
230	$(0.19,\ 0.3)$	3.8×10^{-3}
240	$(0.23,\ 0.31)$	0.07
250	$(0.27,\ 0.31)$	0.36
260	$(0.31,\ 0.31)$	0.87
270	$(0.34,\ 0.31)$	1.59
280	$(0.38,\ 0.32)$	2.51

Table 2: The "best values" of the CKM parameters (ρ, η) as a function of the coupling constant $f_{B_d}\sqrt{\hat{B}_{B_d}}$, obtained by a minimum χ^2 fit to the experimental data, including the renormalized value of $m_t = 170 \pm 11$ GeV. We fix $\hat{B}_K = 1.0$. The resulting minimum χ^2 values from the MINUIT fits are also given.

bit, the values of $f_{B_d}\sqrt{\hat{B}_{B_d}}$ which give the minimum χ^2 values will move around as well. In Tables 3 and 4, we present similar analyses, but for $\hat{B}_K = 0.8$ and 0.6, respectively. From these tables we see that the lower limit on $f_{B_d}\sqrt{\hat{B}_{B_d}}$ remains fairly constant, at around 130 MeV, but the upper limit depends quite strongly on the value of $\hat{B}_K$ chosen. Specifically, for $\hat{B}_K = 0.8$ and 0.6, the maximum allowed value of $f_{B_d}\sqrt{\hat{B}_{B_d}}$ is about 240 and 210 MeV, respectively.

In Table 5, we present the χ^2 values as a function of $f_{B_d}\sqrt{\hat{B}_{B_d}}$ for $\hat{B}_K = 0.4$, which is not favoured by lattice calculations or QCD sum rules. What is striking is that, over the entire range of $f_{B_d}\sqrt{\hat{B}_{B_d}}$, the minimum χ^2 is always greater than 2. This indicates that the data strongly disfavour $\hat{B}_K \leq 0.4$ solutions.

We now discuss the "combined fit" (Fit 2). Since the coupling constants are not known and the best we have are estimates given in the ranges in Eqs. (16) and (21), a reasonable profile of the unitarity triangle at present can be obtained by letting the coupling constants vary in these ranges. The resulting CKM triangle region is shown in Fig. 3. As is clear from this figure, the allowed region is rather large at present. The preferred values obtained from the "combined fit" are

$$(\rho, \eta) = (-0.07, 0.34) \quad (\text{with } \chi^2 = 6.6 \times 10^{-2}) \ . \tag{24}$$

$f_{B_d}\sqrt{\hat{B}_{B_d}}$ (MeV)	(ρ, η)	χ^2_{min}
120	$(-0.42,\ 0.16)$	3.04
130	$(-0.37,\ 0.19)$	1.32
140	$(-0.32,\ 0.23)$	0.43
150	$(-0.27,\ 0.26)$	0.07
160	$(-0.22,\ 0.29)$	1.4×10^{-3}
170	$(-0.15,\ 0.32)$	0.05
180	$(-0.08,\ 0.34)$	0.09
190	$(-0.01,\ 0.35)$	0.06
200	$(0.06,\ 0.35)$	0.01
210	$(0.13,\ 0.35)$	0.02
220	$(0.18,\ 0.35)$	0.2
230	$(0.23,\ 0.35)$	0.61
240	$(0.28,\ 0.35)$	1.29
250	$(0.32,\ 0.35)$	2.22

Table 3: The "best values" of the CKM parameters (ρ, η) as a function of the coupling constant $f_{B_d}\sqrt{\hat{B}_{B_d}}$, obtained by a minimum χ^2 fit to the experimental data, including the renormalized value of $m_t = 170 \pm 11$ GeV. We fix $\hat{B}_K = 0.8$. The resulting minimum χ^2 values from the MINUIT fits are also given.

$f_{B_d}\sqrt{\hat{B}_{B_d}}$ (MeV)	(ρ, η)	χ^2_{min}
120	$(-0.4,\ 0.21)$	3.39
130	$(-0.35,\ 0.25)$	1.7
140	$(-0.29,\ 0.29)$	0.78
150	$(-0.22,\ 0.33)$	0.35
160	$(-0.15,\ 0.36)$	0.18
170	$(-0.07,\ 0.38)$	0.16
180	$(0.01,\ 0.39)$	0.24
190	$(0.08,\ 0.4)$	0.48
200	$(0.15,\ 0.4)$	0.96
210	$(0.21,\ 0.4)$	1.73
220	$(0.26,\ 0.4)$	2.85

Table 4: The "best values" of the CKM parameters (ρ, η) as a function of the coupling constant $f_{B_d}\sqrt{\hat{B}_{B_d}}$, obtained by a minimum χ^2 fit to the experimental data, including the renormalized value of $m_t = 170 \pm 11$ GeV. We fix $\hat{B}_K = 0.6$. The resulting minimum χ^2 values from the MINUIT fits are also given.

$f_{B_d}\sqrt{\hat{B}_{B_d}}$ (MeV)	(ρ, η)	χ^2_{min}
130	$(-0.28,\ 0.35)$	2.95
140	$(-0.2,\ 0.39)$	2.22
150	$(-0.11,\ 0.43)$	2.04
160	$(-0.02,\ 0.45)$	2.32
170	$(0.06,\ 0.46)$	3.07

Table 5: The "best values" of the CKM parameters (ρ, η) as a function of the coupling constant $f_{B_d}\sqrt{\hat{B}_{B_d}}$, obtained by a minimum χ^2 fit to the experimental data, including the renormalized value of $m_t = 170 \pm 11$ GeV. We fix $\hat{B}_K = 0.4$. The resulting minimum χ^2 values from the MINUIT fits are also given.

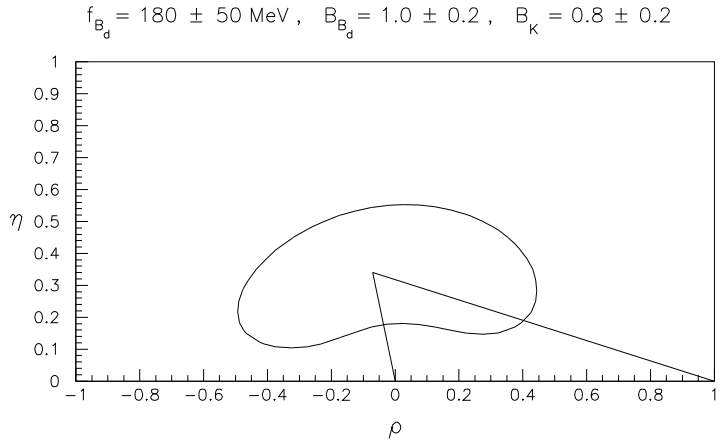

Figure 3: Allowed region in ρ-η space, from a simultaneous fit to both the experimental and theoretical quantities given in Table 1. The theoretical errors are treated as Gaussian for this fit. The solid line represents the region with $\chi^2 = \chi^2_{min} + 6$ corresponding to the 95% C.L. region. The triangle shows the best fit.

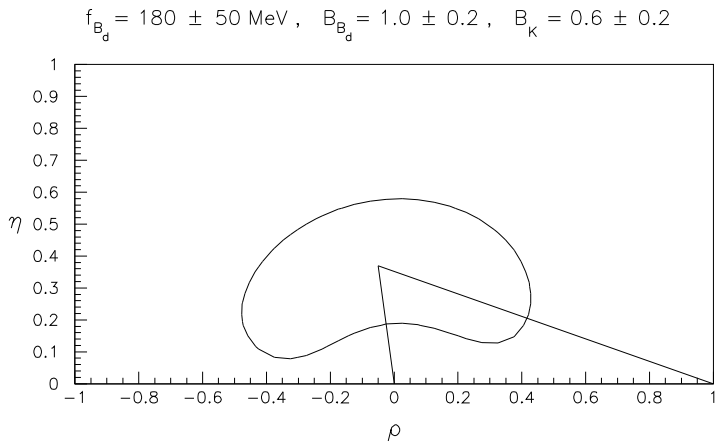

Figure 4: Allowed region in ρ-η space, from a simultaneous fit to both the experimental and theoretical quantities given in Table 1, except that we take $\hat{B}_K = 0.6 \pm 0.2$. The theoretical errors are treated as Gaussian for this fit. The solid line represents the region with $\chi^2 = \chi^2_{min} + 6$ corresponding to the 95% C.L. region. The triangle shows the best fit.

For comparison, we also show the allowed region in the (ρ, η) plane for the case in which $\hat{B}_K = 0.6 \pm 0.2$ [Eq. (17)], which is more favoured by chiral perturbation theory and QCD sum rules. The CKM triangle region is shown in Fig. 4. Clearly, there is not much difference between this figure and Fig. 3. The preferred values obtained from this fit are

$$(\rho, \eta) = (-0.05, 0.37) \quad (\text{with } \chi^2 = 0.1) \; . \tag{25}$$

4 x_s and the Unitarity Triangle

Mixing in the B^0_s-$\overline{B^0_s}$ system is quite similar to that in the B^0_d-$\overline{B^0_d}$ system. The B^0_s-$\overline{B^0_s}$ box diagram is again dominated by t-quark exchange, and the mass difference between the mass eigenstates ΔM_s is given by a formula analogous to that of Eq. (20):

$$\Delta M_s = \frac{G_F^2}{6\pi^2} M_W^2 M_{B_s} \left(f^2_{B_s} \hat{B}_{B_s} \right) \hat{\eta}_{B_s} y_t f_2(y_t) |V^*_{ts} V_{tb}|^2 \; . \tag{26}$$

Using the fact that $|V_{cb}| = |V_{ts}|$ (Eq. 1), it is clear that one of the sides of the unitarity triangle, $|V_{td}/\lambda V_{cb}|$, can be obtained from the ratio of ΔM_d and ΔM_s,

$$\frac{\Delta M_s}{\Delta M_d} = \frac{\hat{\eta}_{B_s} M_{B_s} \left(f^2_{B_s} \hat{B}_{B_s} \right)}{\hat{\eta}_{B_d} M_{B_d} \left(f^2_{B_d} \hat{B}_{B_d} \right)} \left| \frac{V_{ts}}{V_{td}} \right|^2 \; . \tag{27}$$

All dependence on the t-quark mass drops out, leaving the square of the ratio of CKM matrix elements, multiplied by a factor which reflects $SU(3)_{\text{flavour}}$ breaking effects. The only real uncertainty in this factor is the ratio of hadronic matrix elements. Whether

or not x_s can be used to help constrain the unitarity triangle will depend crucially on the theoretical status of the ratio $f_{B_s}^2\hat{B}_{B_s}/f_{B_d}^2\hat{B}_{B_d}$. In what follows, we will take $\xi_s \equiv (f_{B_s}\sqrt{\hat{B}_{B_s}})/(f_{B_d}\sqrt{\hat{B}_{B_d}}) = (1.16 \pm 0.1)$, consistent with both lattice-QCD [36] and QCD sum rules [40]. (The SU(3)-breaking factor in $\Delta M_s/\Delta M_d$ is ξ_s^2.)

The mass and lifetime of the B_s meson have now been measured at LEP and Tevatron and their present values are $M_{B_s} = 5370.0 \pm 2.0$ MeV and $\tau(B_s) = 1.58 \pm 0.10$ ps [28]. We expect the QCD correction factor $\hat{\eta}_{B_s}$ to be equal to its B_d counterpart, i.e. $\hat{\eta}_{B_s} = 0.55$. The main uncertainty in x_s (or, equivalently, ΔM_s) is now $f_{B_s}^2\hat{B}_{B_s}$. Using the determination of A given previously, $\tau_{B_s} = 1.58 \pm 0.10$ (ps) and $\overline{m_t} = 171 \pm 11$ GeV, we obtain

$$\begin{aligned} \Delta M_s &= (13.1 \pm 2.8)\,\frac{f_{B_s}^2\hat{B}_{B_s}}{(230\ \text{MeV})^2}\ (ps)^{-1}\ , \\ x_s &= (20.7 \pm 4.5)\,\frac{f_{B_s}^2\hat{B}_{B_s}}{(230\ \text{MeV})^2}\ . \end{aligned} \tag{28}$$

The choice $f_{B_s}\sqrt{\hat{B}_{B_s}} = 230$ MeV corresponds to the central value given by the lattice-QCD estimates, and with this our fits give $x_s \simeq 20$ as the preferred value in the SM. Allowing the coefficient to vary by $\pm 2\sigma$, and taking the central value for $f_{B_s}\sqrt{\hat{B}_{B_s}}$, this gives

$$\begin{aligned} 11.7 &\leq x_s \leq 29.7\ , \\ 7.5\ (ps)^{-1} &\leq \Delta M_s \leq 18.7\ (ps)^{-1}\ . \end{aligned} \tag{29}$$

It is difficult to ascribe a confidence level to this range due to the dependence on the unknown coupling constant factor. All one can say is that the standard model predicts large values for x_s, most of which are above the present experimental limit $x_s > 8.8$ (equivalently $\Delta M_s > 6.1\ (ps)^{-1}$) [20].

An alternative estimate of ΔM_s (or x_s) can also be obtained by using the relation in Eq. (27). Two quantities are required. First, we need the CKM ratio $|V_{ts}/V_{td}|$. In Fig. 5 we show the allowed values (at 95% C.L.) of the inverse of this ratio as a function of $f_{B_d}\sqrt{\hat{B}_{B_d}}$, for $\hat{B}_K = 0.8 \pm 0.2$. From this one gets

$$2.8 \leq \left|\frac{V_{ts}}{V_{td}}\right| \leq 7.6\ . \tag{30}$$

The second ingredient is the SU(3)-breaking factor which we take to be $\xi_s = 1.16 \pm 0.1$, or $1.1 \leq \xi_s^2 \leq 1.6$. The result of the CKM fit can therefore be expressed as a 95% C.L. range:

$$10.5\left(\frac{\xi_s}{1.16}\right)^2 \ \leq\ \frac{\Delta M_s}{\Delta M_d}\ \leq\ 77.7\left(\frac{\xi_s}{1.16}\right)^2\ . \tag{31}$$

Again, it is difficult to assign a true confidence level to $\Delta M_s/\Delta M_d$ due to the dependence on ξ_s. The large allowed range reflects our poor knowledge of the matrix element ratio $|V_{ts}/V_{td}|$, which shows that this method is not particularly advantageous at present for the determination of the range for ΔM_s.

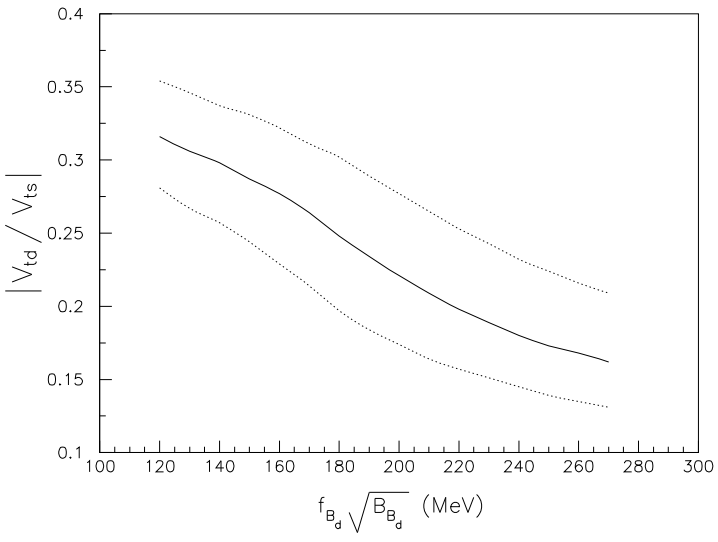

Figure 5: Allowed values of the CKM matrix element ratio $|V_{td}/V_{ts}|$ as a function of the coupling constant product $f_{B_d}\sqrt{\hat{B}_{B_d}}$, for $\hat{B}_K = 0.8 \pm 0.2$. The solid line corresponds to the best fit values and the dotted curves correspond to the maximum and minimum allowed values at 95 % C.L.

The ALEPH lower bound $\Delta M_s > 6.1\ (ps)^{-1}$ (95% C.L.) [20] and the present world average $\Delta M_d = (0.465 \pm 0.024)\ (ps)^{-1}$ can be used to put a bound on the ratio $\Delta M_s/\Delta M_d$. The lower limit on ΔM_s is correlated with the value of f_s, the fraction of b quark fragmenting into B_s meson, as shown in the ALEPH analysis [20]. The value obtained from the measurement of the quantity $f_s BR(B_s \to D_s \ell \nu_\ell)$ is $f_s = (12 \pm 3)\%$. The time-integrated mixing ratios $\bar{\chi}$ and χ_d, assuming maximal mixing in the B_s-$\overline{B_s}$ system $\chi_s = 0.5$, give $f_s = (9 \pm 2)\%$. The weighted average of these numbers is $f_s = (10 \pm 2)\%$ [19]. With $f_s = 10\%$, one gets $\Delta M_s > 5.6\ (ps)^{-1}$ at 95% C.L., yielding $\Delta M_s/\Delta M_d > 11.3$ at 95% C.L. Assuming, however, $f_s = 12\%$ gives $\Delta M_s > 6.1\ (ps)^{-1}$, yielding $\Delta M_s/\Delta M_d > 12.3$ at 95% C.L. We will use this latter number.

The 95% confidence limit on $\Delta M_s/\Delta M_d$ can be turned into a bound on the CKM parameter space (ρ, η) by choosing a value for the SU(3)-breaking parameter ξ_s^2. We assume three representative values: $\xi_s^2 = 1.1$, 1.35 and 1.6, and display the resulting constraints in Fig. 6. From this graph we see that the ALEPH bound marginally restricts the allowed ρ-η region for small values of ξ_s^2, but does not provide any useful bounds for larger values.

Summarizing the discussion on x_s, we note that the lattice-QCD-inspired estimate $f_{B_s}\sqrt{\hat{B}_{B_s}} \simeq 230$ MeV and the CKM fit predict that x_s lies between 12 and 30, with a central value around 20. The upper and lower bounds and the central value scale as $(f_{B_s}\sqrt{\hat{B}_{B_s}}/230\ \text{MeV})^2$. The present constraints from the lower bound on x_s on the CKM parameters are marginal but this would change with improved data. In particular, one expects to reach a sensitivity $x_s \simeq 15$ (or $\Delta M_s \simeq 10\ ps^{-1}$) at LEP combining all data and tagging techniques [19], which would be in the ball-park estimate for this quantity in the SM presented here. Of course, an actual measurement of x_s would be very helpful in

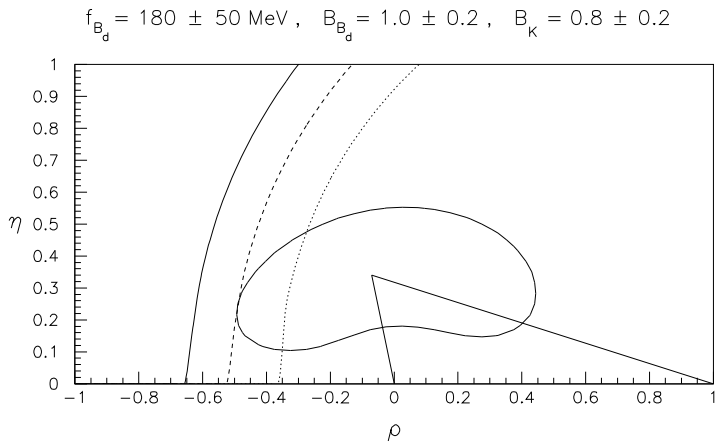

Figure 6: Further constraints in ρ-η space from the ALEPH bound on ΔM_s. The bounds are presented for 3 choices of the SU(3)-breaking parameter: $\xi_s^2 = 1.1$ (dotted line), 1.35 (dashed line) and 1.6 (solid line). In all cases, the region to the left of the curve is ruled out.

further constraining the CKM parameter space.

5 CP Violation in the B System

It is expected that the B system will exhibit large CP-violating effects, characterized by nonzero values of the angles α, β and γ in the unitarity triangle (Fig. 1) [42]. The most promising method to measure CP violation is to look for an asymmetry between $\Gamma(B^0 \to f)$ and $\Gamma(\overline{B^0} \to f)$, where f is a CP eigenstate. If only one weak amplitude contributes to the decay, the CKM phases can be extracted cleanly (i.e. with no hadronic uncertainties). Thus, $\sin 2\alpha$, $\sin 2\beta$ and $\sin 2\gamma$ can in principle be measured in $\overset{(-)}{B_d} \to \pi^+\pi^-$, $\overset{(-)}{B_d} \to J/\psi K_S$ and $\overset{(-)}{B_s} \to \rho K_S$, respectively.

Unfortunately, the situation is not that simple. In all of the above cases, in addition to the tree contribution, there is an additional amplitude due to penguin diagrams [44]. In general, this will introduce some hadronic uncertainty into an otherwise clean measurement of the CKM phases. In the case of $\overset{(-)}{B_d} \to J/\psi K_S$, the penguins do not cause any problems, since the weak phase of the penguin is the same as that of the tree contribution. Thus, the CP asymmetry in this decay still measures $\sin 2\beta$.

For $\overset{(-)}{B_d} \to \pi^+\pi^-$, however, although the penguin is expected to be small with respect to the tree diagram, it will still introduce a theoretical uncertainty into the extraction of α. Fortunately, this uncertainty can be removed by the use of isospin [45]. The key observation is that the $I = 2$ component of the $B \to \pi\pi$ amplitude is pure tree (i.e., it has no penguin contribution) and therefore has a well-defined CKM phase. By measuring the rates for $B^+ \to \pi^+\pi^0$, $B^0 \to \pi^+\pi^-$ and $B^0 \to \pi^0\pi^0$, as well as their CP-conjugate counterparts, it is possible to isolate the $I = 2$ component and obtain α with no theoretical uncertainty. Thus, even in the presence of penguin diagrams, $\sin 2\alpha$ can

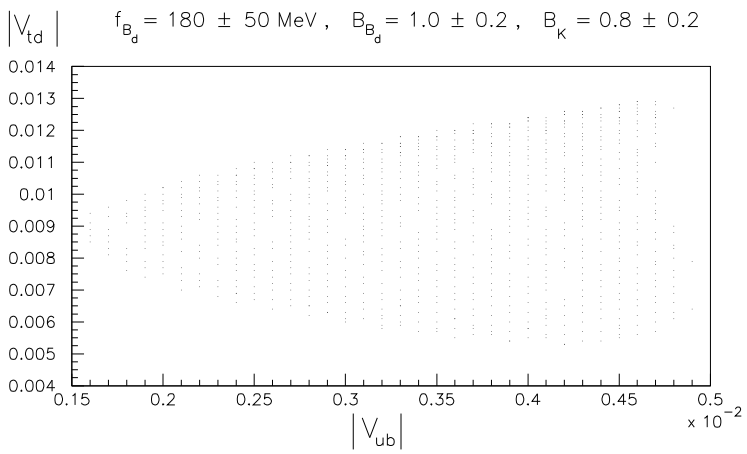

Figure 7: Allowed region of the CKM matrix elements $|V_{td}|$ and $|V_{ub}|$ resulting from the "combined fit" of the data for the ranges for $f_{B_d}\sqrt{\hat{B}_{B_d}}$ and $\hat{B}_K$ given in the text.

in principle be extracted from the decays $B \to \pi\pi$. It must be admitted, however, that this isospin program is ambitious experimentally. If it cannot be carried out, the error induced on $\sin 2\alpha$ is of order $|P/T|$, where P (T) represents the penguin (tree) diagram. The ratio $|P/T|$ is difficult to estimate – it is dominated by hadronic physics. However, one ingredient is the ratio of the CKM elements of the two contributions: $|V_{tb}^* V_{td}/V_{ub}^* V_{ud}| \simeq |V_{td}/V_{ub}|$. From our fits, we have determined the allowed values of $|V_{td}|$ as a function of $|V_{ub}|$. This is shown in Fig. 7 for the "combined fit". The allowed range for the ratio of these CKM matrix elements is

$$1.2 \leq \left|\frac{V_{td}}{V_{ub}}\right| \leq 5.8 \ , \tag{32}$$

with the central value close to 3.

It is $\overset{(-)}{B_s} \to \rho K_S$ which is most affected by penguins. In fact, the penguin contribution is probably larger in this process than the tree contribution. This decay is clearly not dominated by one weak (tree) amplitude, and thus cannot be used as a clean probe of the angle γ. Instead, two other methods have been devised, not involving CP-eigenstate final states. The CP asymmetry in the decay $\overset{(-)}{B_s} \to D_s^{\pm} K^{\mp}$ can be used to extract $\sin^2\gamma$ [46]. Similarly, the CP asymmetry in $B^{\pm} \to D_{CP}^0 K^{\pm}$ also measures $\sin^2\gamma$ [47]. Here, D_{CP}^0 is a D^0 or $\overline{D^0}$ which is identified in a CP-eigenstate mode (e.g. $\pi^+\pi^-$, K^+K^-, ...).

These CP-violating asymmetries can be expressed straightforwardly in terms of the CKM parameters ρ and η. The 95% C.L. constraints on ρ and η found previously can be used to predict the ranges of $\sin 2\alpha$, $\sin 2\beta$ and $\sin^2\gamma$ allowed in the standard model. The allowed ranges which correspond to each of the figures in Fig. 2, obtained from Fit 1, are found in Table 6. In this table we have assumed that the angle β is measured in $\overset{(-)}{B_d} \to J/\Psi K_S$, and have therefore included the extra minus sign due to the CP of the final state.

Since the CP asymmetries all depend on ρ and η, the ranges for $\sin 2\alpha$, $\sin 2\beta$ and $\sin^2\gamma$ shown in Table 6 are correlated. That is, not all values in the ranges are allowed simultaneously. We illustrate this in Fig. 8, corresponding to the "experimental fit" (Fit

$f_{B_d}\sqrt{\hat{B}_{B_d}}$ (MeV)	$\sin 2\alpha$	$\sin 2\beta$	$\sin^2\gamma$
130	0.46 – 0.88	0.21 – 0.37	0.12 – 0.39
155	0.75 – 1.0	0.31 – 0.56	0.34 – 0.92
180	−0.59 – 1.0	0.42 – 0.73	0.68 – 1.0
205	−0.96 – 0.92	0.49 – 0.86	0.37 – 1.0
230	−0.98 – 0.6	0.57 – 0.93	0.28 – 0.97

Table 6: The allowed ranges for the CP asymmetries $\sin 2\alpha$, $\sin 2\beta$ and $\sin^2\gamma$, corresponding to the constraints on ρ and η shown in Fig. 2. Values of the coupling constant $f_{B_d}\sqrt{\hat{B}_{B_d}}$ are stated. We fix $\hat{B}_K = 0.8$. The range for $\sin 2\beta$ includes an additional minus sign due to the CP of the final state $J/\Psi K_S$.

1), by showing the region in $\sin 2\alpha$-$\sin 2\beta$ space allowed by the data, for various values of $f_{B_d}\sqrt{\hat{B}_{B_d}}$. Given a value for $f_{B_d}\sqrt{\hat{B}_{B_d}}$, the CP asymmetries are fairly constrained. However, since there is still considerable uncertainty in the values of the coupling constants, a more reliable profile of the CP asymmetries at present is given by our "combined fit" (Fit 2), where we convolute the present theoretical and experimental values in their allowed ranges. The resulting correlation is shown in Fig. 9. From this figure one sees that the smallest value of $\sin 2\beta$ occurs in a small region of parameter space around $\sin 2\alpha \simeq 0.4$-0.6. Excluding this small tail, one expects the CP-asymmetry in $\overset{(-)}{B}_d \to J/\Psi K_S$ to be at least 30%.

It may be difficult to extract γ using the techniques described above. First, since $\overset{(-)}{B}_s \to D_s^{\pm}K^{\mp}$ involves the decay of B_s mesons, such measurements must be done at hadron colliders. At present, it is still debatable whether this will be possible. Second, the method of using $B^{\pm} \to D^0_{CP}K^{\pm}$ to obtain γ requires measuring the rate for $B^+ \to D^0K^+$. This latter process has an expected branching ratio of $\lesssim O(10^{-6})$, so this too will be hard.

Recently, a new method to measure γ was proposed [48]. Using a flavour SU(3) symmetry, along with the neglect of exchange- and annihilation-type diagrams, it was suggested that γ could be found by measuring rates for the decays $B^+ \to \pi^0K^+$, $B^+ \to \pi^+K^0$, $B^+ \to \pi^+\pi^0$, and their charge-conjugate processes. The πK final states have both $I = 1/2$ and $I = 3/2$ components. The crucial ingredient is that the gluon-mediated penguin diagram contributes only to the $I = 1/2$ final state. Thus, a linear combination of the $B^+ \to \pi^0K^+$ and $B^+ \to \pi^+K^0$ amplitudes, corresponding to $I = 3/2$ in the πK system, can be related via flavour SU(3) to the purely $I = 2$ amplitude in $B^+ \to \pi^+\pi^0$, permitting the construction of an amplitude triangle. The difference in the phase of the $B^+ \to \pi^+\pi^0$ side and that of the corresponding triangle for B^- decays was found to be 2γ. SU(3) breaking can be taken into account by including a factor f_K/f_π in relating $B \to \pi\pi$ decays to the $B \to \pi K$ decays [49].

The key assumption is that the penguin is mediated by gluon exchange. However, there are also electroweak contributions to the penguins [50]. These electroweak penguins (EWP's) are not constrained to be isosinglets. Thus, in the presence of EWP's, there is no longer a triangle relation $B \to \pi K$ and $B \to \pi\pi$ amplitudes [51]. Indeed, electroweak penguins can, in principle, even invalidate the isospin analysis in $B \to \pi\pi$, since the $I = 2$

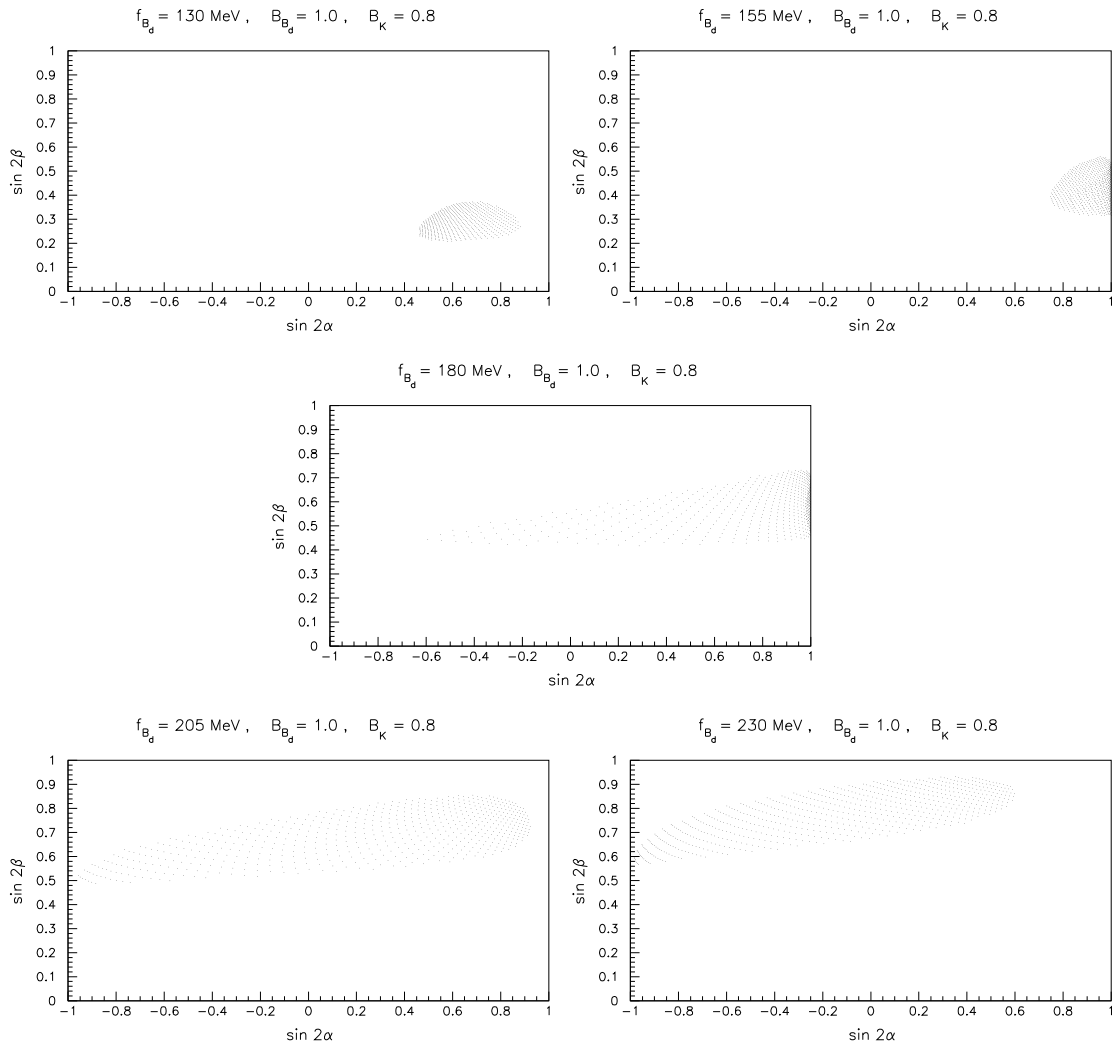

Figure 8: Allowed region of the CP asymmetries $\sin 2\alpha$ and $\sin 2\beta$ resulting from the "experimental fit" of the data for different values of the coupling constant $f_{B_d}\sqrt{\hat{B}_{B_d}}$ indicated on the figures a) – e). We fix $\hat{B}_K = 0.8$.

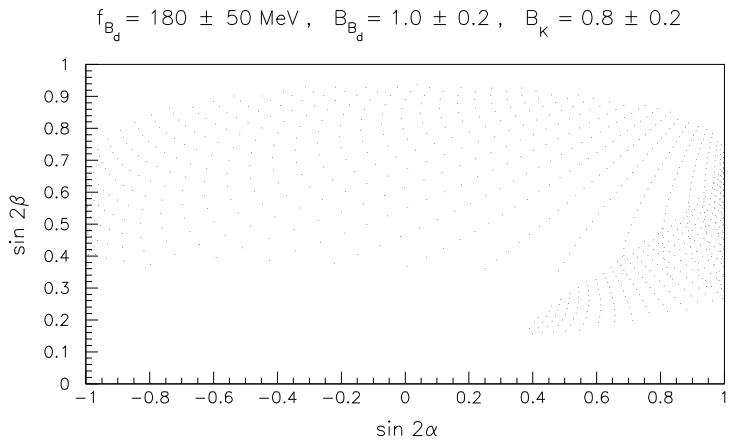

Figure 9: Allowed region of the CP asymmetries $\sin 2\alpha$ and $\sin 2\beta$ resulting from the "combined fit" of the data for the ranges for $f_{B_d}\sqrt{\hat{B}_{B_d}}$ and $\hat{B}_K$ given in the text.

amplitude will include a contribution from EWP's, and hence will no longer have a well-defined weak CKM phase. However, theoretical estimates [51, 52] show that electroweak penguins are expected to be relatively unimportant for $B \to \pi\pi$.

The question of the size of EWP's has therefore become a rather interesting question, and a number of papers have recently appeared discussing this issue [53]. These include both theoretical predictions, as well as ways of isolating EWP's experimentally. The general consensus is that EWP's are large enough to invalidate the method of Ref. [48] for obtaining γ. However, two new methods making use of the flavour SU(3) symmetry, and which do not have any problems with electroweak penguins, have been suggested. Both are rather complicated, making use of the isospin quadrangle relation among $B \to \pi K$ decays, as well as $B^+ \to \pi^+\pi^0$ plus an additional decay: $B_s \to \eta\pi^0$ in one case [52], $B^+ \to \eta K^+$ in the other [54]. Although electroweak penguins do not cause problems, SU(3)-breaking effects which cannot be parametrized simply as a ratio of decay constants are likely to introduce errors of about 25% into both methods. It is clear that this is a subject of great interest at the moment, and work will no doubt continue.

6 Summary and Outlook

We summarize our results:

(i) We have presented an update of the CKM unitarity triangle using the theoretical and experimental improvements in the following quantities: $|V_{cb}|$, $|V_{ub}/V_{cb}|$, ΔM_d, $\tau(B_d)$, $\overline{m_t}$, $\hat{\eta}_{cc}$, $\hat{\eta}_{ct}$. The fits can be used to exclude extreme values of the pseudoscalar coupling constants, with the range 130 MeV $\leq f_{B_d}\sqrt{\hat{B}_{B_d}} \leq$ 270 MeV still allowed for $\hat{B}_K = 1$. The lower limit of this range is quite $\hat{B}_K$-independent, but the upper limit is strongly correlated with the value chosen for $\hat{B}_K$. For example, for $\hat{B}_K = 0.8$ and 0.6, $f_{B_d}\sqrt{\hat{B}_{B_d}} \leq 240$ and 210 MeV, respectively, is required for a good fit. The solutions for $\hat{B}_K = 0.8 \pm 0.2$ are slightly favoured by the data as compared to the lower values. These numbers are

in very comfortable agreement with QCD-based estimates from sum rules and lattice techniques. The statistical significance of the fit is, however, not good enough to determine the coupling constant more precisely. We note that $\hat{B}_K \leq 0.4$ is strongly disfavoured by the data, since the quality of fit for such values is very poor.

(ii) The newest experimental and theoretical numbers restrict the allowed CKM unitarity triangle in the (ρ, η)-space somewhat more than before. However, the present uncertainties are still enormous – despite the new, more accurate experimental data, our knowledge of the unitarity triangle is still poor. This underscores the importance of measuring CP-violating rate asymmetries in the B system. Such asymmetries are largely independent of theoretical hadronic uncertainties, so that their measurement will allow us to accurately pin down the parameters of the CKM matrix. Furthermore, unless our knowledge of the pseudoscalar coupling constants improves considerably, better measurements of such quantities as x_d will not help much in constraining the unitarity triangle. On this point, help may come from the experimental front. It may be possible to measure the parameter f_{B_d}, using isospin symmetry, via the charged-current decay $B_u^\pm \to \tau^\pm \nu_\tau$. With $|V_{ub}/V_{cb}| = 0.08 \pm 0.02$ and $f_{B_d} = 180 \pm 50$ MeV, one gets a branching ratio $BR(B_u^\pm \to \tau^\pm \nu_\tau) = (1.5\text{–}14.0) \times 10^{-5}$, with a central value of 5.2×10^{-5}. This lies in the range of the future LEP and asymmetric B-factory experiments, though at LEP the rate $Z \to B_c X \to \tau^\pm \nu_\tau X$ could be just as large as $Z \to B^\pm X \to \tau^\pm \nu_\tau X$. Along the same lines, the prospects for measuring (f_{B_d}, f_{B_s}) in the FCNC leptonic and photonic decays of B_d^0 and B_s^0 hadrons, $(B_d^0, B_s^0) \to \mu^+\mu^-, (B_d^0, B_s^0) \to \gamma\gamma$ in future B physics facilities are not entirely dismal [55].

(iii) We have determined bounds on the ratio $|V_{td}/V_{ts}|$ from our fits. For 130 MeV $\leq f_{B_d}\sqrt{\hat{B}_{B_d}} \leq 270$ MeV, i.e. in the entire allowed domain, at 95 % C.L. we find

$$0.13 \leq \left|\frac{V_{td}}{V_{ts}}\right| \leq 0.35 \ . \tag{33}$$

The upper bound from our analysis is more restrictive than the current experimental upper limit following from the CKM-suppressed radiative penguin decays $BR(B \to \omega + \gamma)$ and $BR(B \to \rho + \gamma)$, which at present yield at 90% C.L. [56]

$$\left|\frac{V_{td}}{V_{ts}}\right| \leq 0.64 - 0.75 \ , \tag{34}$$

depending on the model used for the SU(3)-breaking in the relevant form factors [57]. Long-distance effects in the decay $B^\pm \to \rho^\pm + \gamma$ may introduce theoretical uncertainties comparable to those in the SU(3)-breaking part but the corresponding effects in the decays $B^0 \to (\rho^0, \omega) + \gamma$ are expected to be very small [58]. Furthermore, the upper bound is now as good as that obtained from unitarity, which gives $0.08 \leq |V_{td}/V_{ts}| \leq 0.36$, but the lower bound from our fit is more restrictive.

(iv) Using the measured value of m_t, we find

$$x_s = (20.7 \pm 4.5)\, \frac{f_{B_s}^2 \hat{B}_{B_s}}{(230 \text{ MeV})^2} \ . \tag{35}$$

Taking $f_{B_s}\sqrt{\hat{B}_{B_s}} = 230$ (the central value of lattice-QCD estimates), and allowing the coefficient to vary by $\pm 2\sigma$, this gives

$$11.7 \leq x_s \leq 29.7 \ . \tag{36}$$

No reliable confidence level can be assigned to this range – all that one can conclude is that the SM predicts large values for x_s, most of which lie above the ALEPH 95% C.L. lower limit of $x_s > 8.8$.

(v) The ranges for the CP-violating rate asymmetries parametrized by $\sin 2\alpha$, $\sin 2\beta$ and and $\sin^2\gamma$ are determined at 95% C.L. to be

$$\begin{aligned} -1.0 \leq \sin 2\alpha \leq 1.0 \ , \\ 0.21 \leq \sin 2\beta \leq 0.93 \ , \\ 0.12 \leq \sin^2\gamma \leq 1.0 \ . \end{aligned} \tag{37}$$

(For $\sin 2\alpha < 0.4$, we find $\sin 2\beta \geq 0.3$.) Electroweak penguins may play a significant role in some methods of extracting γ. Their magnitude, relative to the tree contribution, is therefore of some importance. One factor in determining this relative size is the ratio of CKM matrix elements $|V_{td}/V_{ub}|$. We find

$$1.2 \leq \left|\frac{V_{td}}{V_{ub}}\right| \leq 5.8 \ . \tag{38}$$

Acknowledgements:

We thank Viladimir Braun, Roger Forty, Christoph Greub, Matthias Neubert, Olivier Schneider, Vivek Sharma, Tomasz Skwarnicki, Ed Thorndike, Pippa Wells and Sau Lan Wu for very helpful discussions. A.A. thanks the hospitality of the organizing committee for the 6^{th} symposium on heavy flavour physics in Pisa.

References

[1] ALI, A. and LONDON, D., *Z. Phys.,* C65 (1995) 431.

[2] NEUBERT, M., Preprint CERN-TH/95-107 (hep-ph/9505238).

[3] SHIFMAN, M., Preprint TPI-MINN-95/15-T (hep-ph/9505289).

[4] HERRLICH, S. and NIERSTE, U., Preprint TUM-T31-81/95 (hep-ph/9507262).

[5] ABE, F. et al. (CDF Collaboration), *Phys. Rev.,* D50 (1994) 2966, *Phys. Rev. Lett.,* 73 (1994) 225, *Phys. Rev.,* D51 (1995) 4623.

[6] ABE, F. et al. (CDF Collabaration), Preprint Fermilab-Pub-94/022-E (hep-ex/9503002).

[7] ABACHI, S. et al. (D0 Collaboration), Preprint Fermilab-Pub-95/028-E (hep-ex/9503003).

[8] BELLETINI, G., these proceedings.

[9] GRAY, N., BROADHURST, D.J., GRAFE, W. and SCHILCHER, K., *Z. Phys.,* C48 (1990) 673.

[10] BUSKULIC, D. et al. (ALEPH Collaboration), CERN-PPE/95-094 (1995).

[11] SCOTT, I.J. (ALEPH Collaboration), in: *Proc. of the XXVII Int. Conf. on High Energy Physics*, Glasgow, Scotland, July 1994, edited by P.J. BUSSEY and I.G. KNOWLES (IOP Publications Ltd., Bristol, 1995), Vol. 2, p. 1121.

[12] BROWDER, T.E. (CLEO Collaboration), in: *Proc. of the XXVII Int. Conf. on High Energy Physics*, Glasgow, Scotland, July 1994, edited by P.J. BUSSEY and I.G. KNOWLES (IOP Publications Ltd., Bristol, 1995), Vol. 2, p.1117.

[13] ALBRECHT, H. et al. (ARGUS Collaboration), *Z. Phys.,* C57 (1993) 533; SCHRÖDER, H. (private communication).

[14] BLOCH, D. et al. (DELPHI Collaboration), Contributed paper (eps0569) to the EPS-HEP Conference, Brussels, July 27 - August 2, 1995.

[15] SHIFMAN, M., URALTSEV, N.G. and VAINSHTEIN, A., *Phys. Rev.,* D51 (1995) 2217.

[16] PATTERSON, R., in: *Proc. of the XXVII Int. Conf. on High Energy Physics*, Glasgow, Scotland, July 1994, edited by P.J. BUSSEY and I.G. KNOWLES (IOP Publications Ltd., Bristol, 1995), Vol. 1, p.149.

[17] THORNDIKE, E. (CLEO Collaboration), in "Heavy Flavour Physics" session (PA14), EPS-HEP Conference, Brussels, July 27-August 2, 1995.

[18] See, for example, BURAS, A.J. and HARLANDER, M.K. in *Heavy Flavours*, edited by A.J. BURAS and M. LINDNER, Advanced Series on Directions in High Energy Physics (World Scientific, Singapore, 1992), Vol. 10.

[19] WELLS, P. (OPAL Collaboration), invited talk in the "Heavy Flavour Physics" session (PA14); SCHNEIDER, O. (ALEPH Collaboration), in the "CP Violation, CKM Matrix and Rare Decays" session (PA5); ALEKSAN, R., Plenary talk, EPS-HEP Conference, Brussels, July 27-August 2, 1995.

[20] BUSKULIC, D. et al. (ALEPH Collaboration), CERN-PPE/95-084 (1995).

[21] WOLFENSTEIN, L., *Phys. Rev. Lett.,* 51 (1983) 45.

[22] MONTANET, L. et al. (Particle Data Group), *Phys. Rev.,* D50 (1994) 1173.

[23] ISGUR, N. and WISE, M., *Phys. Lett.,* B232 (1989) 113; 237 (1990) 527.

[24] LUKE, M.E., *Phys. Lett.,* B252 (1990) 447.

[25] BOYD, C.G. and BRAHM, D.E., *Phys. Lett.,* B257 (1991) 393.

[26] NEUBERT, M. and RIECKERT, V., *Nucl. Phys.*, B382 (1992) 97; NEUBERT, M., *Phys. Lett.,* B264 (1991) 455, *Phys. Rev.,* D46 (1992) 2212.

[27] VOLOSHIN, M.B. and SHIFMAN, M.A., *Sov. J. Nucl. Phys.* 45 (1987) 292.

[28] KOMAMIYA, S., Plenary talk, EPS-HEP Conference, Brussels, July 27 - August 2, 1995.

[29] BOYD, C.G., GRINSTEIN, B. and LEBED, R.F., Preprint UCSD/PTH 95-03 (hep-ph/9504235); Preprint UCSD/PTH 95-11 (hep-ph/9508211).

[30] ISGUR, N., SCORA, D., GRINSTEIN, B. and WISE, M., *Phys. Rev.,* D39 (1989) 799.

[31] BURAS, A.J., SŁOMINSKI, W. and STEGER, H., *Nucl. Phys.*, B238 (1984) 529; B245 (1984) 369.

[32] HERRLICH, S. and NIERSTE, U., *Nucl. Phys.*, B419 (1994) 292.

[33] BURAS, A.J., JAMIN, M. and WEISZ, P.H., *Nucl. Phys.*, B347 (1990) 491.

[34] FLYNN, J., *Mod. Phys. Lett.*, A5 (1990) 877.

[35] ALI, A. and LONDON, D., *J. Phys. G: Nucl. Part. Phys.* 19 (1993) 1069.

[36] SHIGEMITSU, J., in: *Proc. of the XXVII Int. Conf. on High Energy Physics*, Glasgow, Scotland, July 1994, edited by P.J. BUSSEY and I.G. KNOWLES (IOP Publications Ltd., Bristol, 1995).

[37] GAVELA, M.B. et al., *Phys. Lett.,* B206 (1988) 113; *Nucl. Phys.*, B306 (1988) 677; BERNARD, C. and SONI, A., *Nucl. Phys. B (Proc. Suppl.)* 17 (1990) 495; KILCUP, G.W., SHARPE, S.R., GUPTA, R. and PATEL, A., *Phys. Rev. Lett.,* 64 (1990) 25; GUPTA, R. et al., *Phys. Rev.,* D47 (1993) 5113; SHARPE, S.R., *Nucl. Phys. B (Proc. Suppl.)*, 34 (1994) 403.

[38] PICH, A. and PRADES, J., Preprint FTUVC/94-37,IFIC/94-32,NBI-94/32 (1994).

[39] BURAS, A.J., LAUTENBACHER, M.E. and OSTERMAIER, G., *Phys. Rev.,* D50 (1994) 3433.

[40] NARISON, S., *Phys. Lett.,* B322 (1994) 247; NARISON, S. and PIVOVAROV, A., *Phys. Lett.,* B327 (1994) 341.

[41] SOMMER, R., DESY Report 94-011 (1994).

[42] For reviews, see, for example, NIR, Y. and QUINN, H.R., in *B Decays*, edited by S. STONE (World Scientific, Singapore, 1992), p. 362; DUNIETZ, I., *ibid* p. 393.

[43] ALEKSAN, R., KAYSER, B. and LONDON, D., *Phys. Rev. Lett.,* 73 (1994) 18.

[44] LONDON, D. and PECCEI, R., *Phys. Lett.,* B223 (1989) 257; GRINSTEIN, B., *Phys. Lett.,* B229 (1989) 280; GRONAU, M., *Phys. Rev. Lett.,* 63 (1989) 1451, *Phys. Lett.,* B300 (1993) 163.

[45] GRONAU, M. and LONDON, D., *Phys. Rev. Lett.,* 65 (1990) 3381.

[46] ALEKSAN, R., DUNIETZ, I. and KAYSER, B., *Z. Phys.,* C54 (1992) 653.

[47] GRONAU, M. and WYLER, D., *Phys. Lett.,* B265 (1991) 172. See also GRONAU, M. and LONDON, D., *Phys. Lett.,* B253 (1991) 483; DUNIETZ, I., *Phys. Lett.,* B270 (1991) 75.

[48] GRONAU, M., ROSNER, J.L. and LONDON, D., *Phys. Rev. Lett.,* 73 (1994) 21. See also HERNÁNDEZ, O.F., LONDON, D., GRONAU, M. and ROSNER, J.L. *Phys. Lett.,* B333 (1994) 500, GRONAU, M., LONDON, D., HERNÁNDEZ, O.F. and ROSNER, J.L., *Phys. Rev.,* D50 (1994) 4529; BURAS A.J. and FLEISCHER, R., hep-ph/9409244, August 1994.

[49] GRONAU, M., LONDON, D., HERNÁNDEZ, O.F. and ROSNER, J.L., hep-ph/9504326, March, 1995, to be published in *Phys. Rev. D.*

[50] FLEISCHER, R., *Z. Phys.,* C62 (1994) 81, *Phys. Lett.,* B321 (1994) 259, 332, (1994) 419.

[51] DESHPANDE, N.G. and HE, X.-G., *Phys. Rev. Lett.,* 74 (1995) 26.

[52] GRONAU, M., LONDON, D., HERNÁNDEZ, O.F. and ROSNER, J.L., hep-ph/9504327, April, 1995.

[53] FLEISCHER, R., *Phys. Lett.,* B332 (1994) 419; DESHPANDE, N.G., HE, X.-G. and TRAMPETIC, J., *Phys. Lett.,* B345 (1995) 547; KRAMER, G. and PALMER, W.F., hep-ph/9507329, July 1995; BURAS A.J. and FLEISCHER, R., hep-ph/9507303, July 1995.

[54] DESHPANDE, N.G. and HE, X.-G., hep-ph/9505369, May 1995.

[55] ALI, A., in *B Decays*, Revised 2nd edition, edited by S. STONE (World Scientific, Singapore, 1994), p. 1.

[56] ATHANAS, M. et al. (CLEO Collaboration), CLEO CONF 94-2 (1994).

[57] ALI, A., BRAUN, V.M. and SIMMA, H., *Z. Phys.,* C63 (1994) 437; SOARES, J.M., *Phys. Rev.,* D49 (1994) 283; NARISON, S., *Phys. Lett.,* B327 (1994) 354.

[58] ALI, A. and BRAUN, V.M., DESY Report 95-106 (1995) (hep-ph/9506248); KHODJAMIRIAN, A., STOLL, G. and WYLER, D., Preprint ZU-TH 8/95, LMU 06/95 (hep-ph/9506242).